[PROC. OF JSCE Structural Eng./Earthquake Eng. Vol. 2, No. 2 October 1985]

STRESS ANALYSIS OF A CRACK AT AN END OF PARTLY EMBEDDED STRIP

By Norio HASEBE and Masahiko MIURA***

Stress analysis is carried out for a strip whose part is embedded and with a crack which emanates at a stiffened end between the embedded and unembedded parts. As loading conditions, a uniaxial tension and a bending in a plane of the strip are considered. Stress distribution before and after the occurrence of a crack is investigated. In particular, stress intensity factor for some crack length and Poisson's ratio is investigated. Stress analysis is carried out as a mixed boundary value problem in the plane elastic problem. Complex variable method and a rational mapping function of fractional expressions are used. A closed solution can be obtained for the rational mapping function.

1. INTRODUCTION

Many analyses have been carried out for cracks emanating from parts of stress concentration. However most of them are for cracks which occur at parts of stress concentration of geometrical shape. In this paper, stress analysis is carried out for a strip whose part is embedded and with a crack which emanates at a stiffened end between the embedded and unembedded parts. This is also a model for a strip which is stiffened on its boundary by rigid plates and with a crack at a stiffened end. If young's modulus of welding material is much larger than that of the strip, this model is that of a crack occuring at the weld toe. An infinite stress occurs at such a stiffened end and a crack may occur. Therefore it seems meaningfull to analyze stress of such a model.

One of the authors analyzed stress of an embedded strip with two cracks at both stiffened ends between an embedded and unembedded parts[1]. He also analyzed a semi-infinite plate whose part on the boundary is stiffened rigidly and which has a crack at a stiffened end of the stiffener[2),3)]. F. Delale et al. analyzed a semi-infinite plate with a crack at an end of an elastic stiffener[4)].

As loading conditions, a uniaxial tension and a bending in a plane of the strip are considered. Stress distribution before and after the occurrence of a crack is investigated. In particular stress intensity factor for some crack length and Poisson's ratio is investigated. Stress analysis is carried out as a mixed boundary value problem. Complex variable method and a rational mapping function of a sum of fractional expressions are used. A closed solution can be obtained for the rational mapping function. It is exact for a shape represented by the rational mapping function.

* Member of JSCE, Dr. Eng., Professor, Dept. of Civil Eng., Nagoya Institute of Tech. (Gokisocho, Showaku, Nagoya 466, Japan)

** Member of JSCE, M. Eng., Chubu Electric Power Co. (Tosincho 10-1, Higashiku, Nagoya 461, Japan)

2. MAPPING FUNCTION

A mapping function which maps a strip region with a crack into a unit circle is formed (see Fig. 1). This function can be obtained by Schwarz Christoffel's transformation, i. e.

$$z=K\int\frac{\zeta-1}{(\zeta^2+1)(\zeta-e^{-i\gamma})^{0.5}(\zeta-e^{i\gamma})^{0.5}}\,d\zeta=\frac{-iK}{2\sqrt{\cos\gamma}}\left[\log\frac{\zeta+i}{\zeta-i}\right.$$
$$\left.+\log\left\{\frac{\zeta(i-\cos\gamma)-i\cos\gamma+1-\sqrt{-2i\cos\gamma(\zeta^2-2\zeta\cos\gamma+1)}}{-\zeta(i+\cos\gamma)+i\cos\gamma+1-\sqrt{2i\cos\gamma(\zeta^2-2\zeta\cos\gamma+1)}}\right\}\right] \quad \cdots\cdots (1)$$

The coefficient K is determined such that the strip width is W, i. e. $K=2Wi\cos(\gamma/\pi)$ where the imaginary unit "i" is used in order that the strip is in the direction of the x axis. The parameter γ relates to the crack length b and is determined by the following equation,

$$\gamma=\begin{cases}\cos^{-1}\left\{\dfrac{(3T^2+4)+4\sqrt{T^2+1}}{9T^2+8}\right\} & 0\le b/w\le 0.5\\ \cos^{-1}\left\{\dfrac{(3T^2+4)-4\sqrt{T^2+1}}{9T^2+8}\right\} & 0.5\le b/w\le 1.0\end{cases}$$

in which $T=-\tan(b\pi/W)$. When $\gamma=0$, Eq. (1) shows the strip region without a crack.

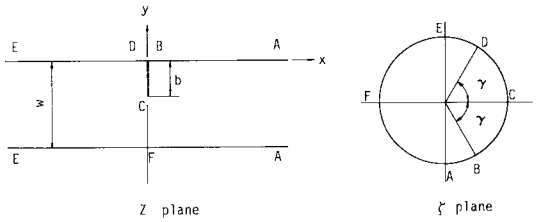

Fig. 1 Region on the z plane and a Unit Circle.

A rational mapping function of a sum of fractional expressions is formed from Eq. 1). The formulation is briefly stated because it has been described in Refs. 5), 6), 7). Eq. (1) is separated into terms which have slow convergence and rapid convergence,

$$Z/K=\frac{A}{2}\int\frac{d\zeta}{1-i\zeta}+\frac{A}{2}\int\frac{d\zeta}{1+i\zeta}+\int\frac{C}{(e^{-i\gamma}-\zeta)^{0.5}}\,d\zeta+\int\frac{D}{(e^{i\gamma}-\zeta)^{0.5}}\,d\zeta$$
$$+\int\left\{\frac{1-\zeta}{(1+\zeta^2)(e^{-i\gamma}-\zeta)^{0.5}(e^{i\gamma}-\zeta)^{0.5}}-\frac{A}{1+\zeta^2}-\frac{C}{(e^{-i\gamma}-\zeta)^{0.5}}-\frac{D}{(e^{i\gamma}-\zeta)^{0.5}}\right\}d\zeta \quad \cdots\cdots (2)$$

where coefficients A, C and D are given by the following expressions,

$$A=\frac{1}{\sqrt{\cos\gamma}},\quad C=\overline{D}=\frac{1-e^{-i\gamma}}{(1+e^{-2i\gamma})\sqrt{2i\sin\gamma}}$$

The following fractional expression is considered for the first term in Eq. (2).

$$\int\frac{d\zeta}{1-i\zeta}=i\log(1-i\zeta)\fallingdotseq-i\sum_{j=1}^{14}\left(\frac{B_j}{1-i\beta_j\zeta}-B_j\right) \quad \cdots\cdots (3)$$

The procedure to determine coefficients B_j and β_j is described in Refs. 7), 6), 5) and the values are shown in Ref. 1. A fractional expression for the second term in Eq. (2) is obtained by exchanging "i" in Eq. (3) for "$-i$" (see Eq. 5). For the third term in Eq. (2), the following fractional expression is considered,

$$\int\frac{d\zeta}{(e^{-i\gamma}-\zeta)^{0.5}}=-2e^{-0.5i\gamma}(1-e^{i\gamma}\zeta)^{0.5}\approx-2e^{-0.5i\gamma}\left[1+\sum_{j=1}^{12}\left(\frac{-A_j}{1-e^{i\gamma}\alpha_j\zeta}+A_j\right)\right] \quad \cdots\cdots (4)$$

The procedure to determine A_j and α_j is also described in Refs. 7,) 6), 5) and the values are shown in Ref. 1). A fractional expression for the fourth term in Eq. (2) is obtained by exchanging "i" in Eq. (4) for "$-i$". For the final integral term in Eq. (2), the following fractional expression is considered,

$$\text{Integral term}\approx\sum_{j=1}^{m}\frac{G_j\gamma_j\zeta}{1-\gamma_j\zeta}$$

The procedure to determine G_j and γ_j is also described in Refs. 7), 6), 5). In this paper, the number of $m=10\sim18$ is adopted. From the formulation above, the following rational mapping function is obtained for Eq. (1),

$$z=\omega(\zeta)=K\left\{A\sum_{j=1}^{14}\frac{B_j\beta_j\zeta}{1+\beta_j^2\zeta^2}+2\,Ce^{-0.5i\gamma}\sum_{j=1}^{12}\frac{A_j\alpha_j e^{i\gamma}\zeta}{1-\alpha_j e^{i\gamma}\zeta}+2\,De^{0.5i\gamma}\sum_{j=1}^{12}\frac{A_j\alpha_j e^{-i\gamma}\zeta}{1-\alpha_j e^{-i\gamma}\zeta}+\sum_{j=1}^{m}\frac{G_j\gamma_j\zeta}{1-\gamma_j\zeta}\right\}$$
$$\equiv\sum_{k=1}^{52+m}\frac{E_k}{\zeta_k-\zeta}+\text{Constant} \quad (5)$$

The constant term in Eq. (5) is determined such that the x and y axes hold the position as shown in Fig. 1. Because Eq. (5) is rational, the strip length is finite and is about 9.6 times of the width. The tip of the crack and points D and B have a round corner. However the radius of curvature of the tip is $\rho/W=10^{-5}\sim10^{-11}$ while depending on the crack length. The radius of curvature is small. The fractional expression regarding to B_j and β_j in Eq. (5) is the rational mapping function for the strip region without a crack.

3. ANALYTICAL METHOD AND BOUNDARY CONDITION

A complex variable method is used for a solution of the mixed boundary value problem. The analytical method has been described in Ref. 2). Therefore necessary equations are only stated. Analytical complex functions are shown by $\phi(\zeta)$ and $\psi(\zeta)$. The part of boundary which external forces are given is shown by L and by M the part which displacements are given. In this paper, L is the part FABCD and M is DEF in Fig. 1. Functions $\phi(\zeta)$ and $\psi(\zeta)$ are given by the following equations,

$$\phi(\zeta)=-\chi(\zeta)\sum_{k=1}^{52+m}\frac{\bar{A}_kC_k}{\chi(\zeta_k)(\zeta_k-\zeta)}+H(\zeta) \quad (6)$$

$$H(\zeta)=M(\zeta)-\frac{\varkappa+1}{2\pi i x}\chi(\zeta)\int_M\frac{M(\sigma)}{\chi(\sigma)(\sigma-\zeta)}\,d\sigma \quad (7)$$

$$M(\zeta)=\frac{1}{2\pi i}\int_{L+M}\frac{f(\sigma)}{\sigma-\zeta}\,d\sigma \quad (8)$$

$$f(\sigma)=\begin{cases} i\int[p_x(s)+ip_y(s)]ds & \text{on } L \\ -2\,G(u+iv) & \text{on } M \end{cases} \quad (9)$$

$$\psi(\zeta)=\frac{1}{2\pi i}\int_{L+M}\frac{\overline{f(\sigma)}}{\sigma-\zeta}\,d\sigma-\overline{\phi(0)}+\frac{\varkappa+1}{2\pi i}\int_M\frac{\bar{\phi}(1/\sigma)}{\sigma-\zeta}\,d\sigma-\frac{\bar{\omega}(1/\zeta)}{\omega'(\zeta)}\phi'(\zeta)-\sum_{k=1}^{52+m}\frac{A_k\bar{C}_k\zeta_k'^2}{\zeta_k'-\zeta} \quad (10)$$

The function $\chi(\zeta)$ is the Plemelj function and is given by $(\zeta-\alpha)^m(\zeta-\beta)^{1-m}$ in which α and β are coordinates on the unit circle at joints of L and M. In this paper α and β show points D and F in Fig. 1 and $\alpha=e^{i\gamma}$ and $\beta=-1$. The index m in $\chi(\zeta)$ is $m=0.5-i(\log\varkappa)/(2\pi)$. $\varkappa$ is $\varkappa=3-4\nu$ for the plane strain and $\varkappa=(3-\nu)/(1+\nu)$ for the generalyzed plane stress and ν is a Poisson's ratio. Coefficients C_k in Eq. 6 are given by $C_k\equiv E_k/\overline{\omega'(\zeta_k)}$ $(k=1, 2, \cdots, 52+m)$ and ζ_k' is $\zeta_k'\equiv1/\bar{\zeta}_k$, the reflection point of ζ_k on the unit circle. A_k and $\bar{A}_k$ are determined by solving simultaneous linear equations of $2(52+m)$. σ in Eq. (7) means ζ on the unit circle. $p_x(s)$ and $p_y(s)$ in Eq. (9) are external forces on L in the direction of the x and y axes respectively. The integration with respect to s means that along the boundary line. u and v in Eq. (9) are displacements in the direction of the x and y axes on M respectively. G is a shear modulus.

As loading conditions, a uniaxial tension in the direction of the strip and a bending in the plane are considered (see Figs. 4, 5).

a) Uniaxial tension

A concentrated load P acts at the tip of the strip, i.e., $\zeta=-i$ on the unit circle. The following boundary equations are obtained from Eq. (9).

$$\begin{aligned} i\int[p_x(s)+ip_y(s)]ds&=0 \quad \text{on FA} \\ &=iP \quad \text{on ABCD} \\ u+iv&=0 \quad \text{on DEF} \end{aligned} \quad (11)$$

If Eq. (11) is substituted into Eq. (8), $M(\zeta)=(P/2\pi)\log[(\zeta-\alpha)/(\zeta+i)]$ can be obtained. Further $M(\zeta)$ is substituted into Eq. (7) and an integral of the second term has to be carried out, but the integral seems difficult. However the first derivative $H'(\zeta)$ of Eq. (7) has been obtained as the following equation[3],

$$H'(\zeta)=(P/2\pi)(i+\alpha)^{1-m}(i+\beta)^{m}(\zeta-\alpha)^{m-1}(\zeta-\beta)^{-m}(i+\zeta)^{-1} \quad (12)$$

Therefore the first derivative $\phi'(\zeta)$ of Eq. (6) can be obtained without an integral term.

b) Bending in the plane

A couple $M=P\varepsilon$ acts at the tip of the strip. P is a pair of the forces with the same magnitude and the opposite direction and ε is a distance between applied points of P. If coordinates on the unit circle where a pair of the forces P acts are expressed by $\zeta=s_1$ and $\zeta=s_2$, the expression $M(\zeta)$ of Eq. (8) is $M(\zeta)=(P/2\pi)\log[(s_1-\zeta)/(s_2-\zeta)]$. When this expression $M(\zeta)$ is substituted into Eq. (7), the integral of the second term is also difficult. However the first derivative of $H(\zeta)$ can be given by the following expression as well Eq. (12),

$$H'(\zeta)=\frac{M}{2\pi\varepsilon}\left\{\frac{(s_2-\alpha)^{1-m}(s_2-\beta)^{m}}{s_2-\zeta}-\frac{(s_1-\alpha)^{1-m}(s_1-\beta)^{m}}{s_1-\zeta}\right\}(\zeta-\alpha)^{m-1}(\zeta-\beta)^{-m} \quad (13)$$

In order to obtain the another function $\psi(\zeta)$, the integral of the third term in Eq. (10) must be carried out. However it can not be carried out because the function $\phi(\zeta)$ is unknown. Using the theorem of analytic continuation[8], $\psi(\zeta)$ can be obtained as follows;

$$\psi(\zeta)=-\overline{\phi}(1/\zeta)-\frac{\overline{\omega}(1/\zeta)}{\omega'(\zeta)}\phi'(\zeta) \quad (14)$$

4. STRESS DISTRIBUTION

A solution for the unembedded strip can be obtained if parameters α and β in Eq. (6) are approached to "i". Figs. 2 and 3 show examples of stress distribution with crack length $b/w=0.4$ for a uniaxial tension and a bending respectively. A solution can be obtained before the occurrence of a crack of the embedded strip,

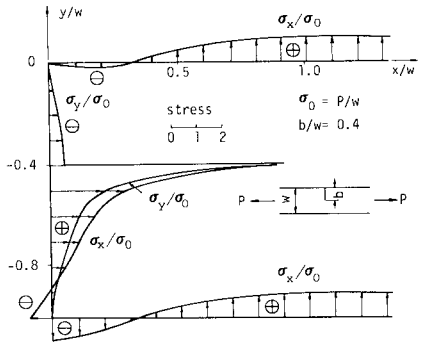

Fig. 2 Example of Stress Distribution of an Unembedded Strip under Tension.

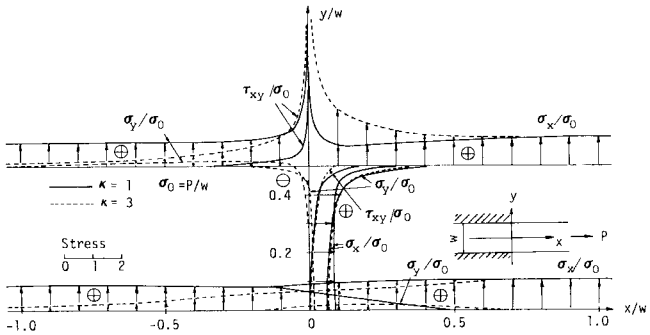

Fig. 4 Stress Distribution before the Occurrence of a Crack under Tension.

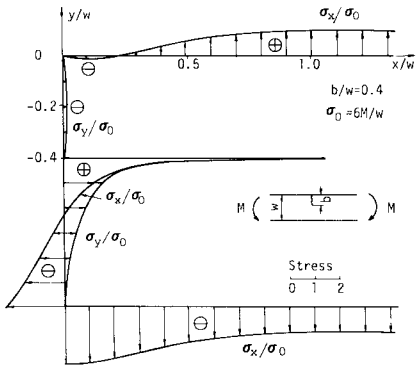

Fig. 3 Example of Stress Distribution of an Unembedded Strip under Bending.

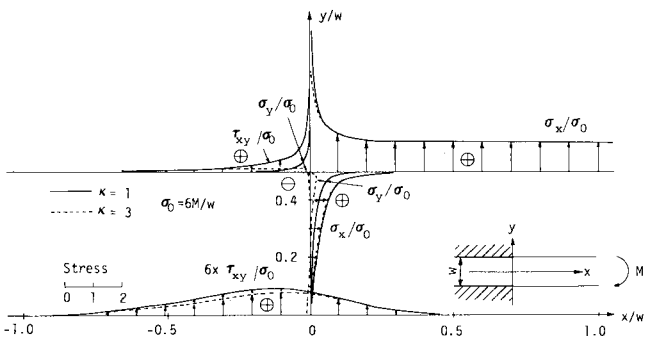

Fig. 5 Stress Distribution before the Occurrence of a Crack under Bending.

if the term $\sum B_i\beta_i/(1+\beta_j^2\zeta^2)$ in Eq. (5) is used as the mapping function and $\alpha=1$ and $\beta=-1$ are put. Figs. 4 and 5 show the stress distribution for $\varkappa=1$ and $\varkappa=3$ before the occurrence of a crack. $\varkappa=1$ corresponds to $\nu=0.5$ for the plane strain and $\varkappa=3$ to $\nu=0$ for the plane strain and the generalyzed plane stress. There is the following relation between σ_θ and σ_r on the boundary M, i.e. $\sigma_\theta/\sigma_r=(3-\varkappa)/(1+\varkappa)$ (Ref. 2)). σ_θ is a tangential stress and σ_r is a normal stress with respect to a curvilinear coordinate which is represented by the mapping function. $\sigma_\theta=\sigma_x$ and $\sigma_r=\sigma_y$ on $y=w/2$ and $y=-w/2$ in Figs. 4 and 5. Large stress concentration occurs at stiffened ends between the boundary M and L. It is noted there are difference between stress distribution for $\varkappa=1$ and $\varkappa=3$. It is noted from Fig. 4 that stresses for $\varkappa=1$ become $\sigma_x=\sigma_y=0.866\,\sigma_0$ on the boundary of the embedded part when $x\to-\infty$. On the other hand, stresses for $\varkappa=3$ become small when $x\to-\infty$. When $\varkappa=1$, the Poisson's ratio is $\nu=0.5$ and so bulk strain is zero. The stress condition is symmetric about the x axis. The width of the strip is unchanged because the displacement on the boundary M is zero. Therefore stresses do not decrease when $x\to-\infty$. In the case of a bending, the influence of $\varkappa$ on the stress distribution is smaller than that of a uniaxial tension. Stresses for any $\varkappa$ become small when $x\to-\infty$. This is because the stress condition is antisymmetric about the x axis and the deformation in the direction of the width w is small. Figs. 6 and 7 show examples of stress distribution with the crack length $b/w=0.4$ for a uniaxial tension and a bending respectively. It is found from Fig. 6 that compression stress occurs on the boundary $y/w=-1$ and $|x/w|<0.3$ because the neutral axis is eccentric for the crack. Stress distribution on the embedded part is different between $\varkappa=1$ and 3. Stress σ_y on the boundary for $\varkappa=1$ approaches 1.451 σ_0 when $x\to-\infty$. The value of stress increases about 45 % than nominal stress σ_0 and is larger than the value $\sigma_y=1.121\,\sigma_0$ before the occurrence of a crack. The resultant force on the section of $x/w=0$ is the same as the external force P before and after the occurrence of a crack while their stress distribution and their deformation near $x/w=0$ are different. When $\varkappa=1$, $\nu=0.5$ and so the bulk strain is zero. Accordingly the situation on the embedded part is determined by the stress condition near $x/w=0$ and stresses σ_x and σ_y on the boundary for $\varkappa=1$ do not decrease when $x\to-\infty$. It is found from Fig. 7 that the influence of $\varkappa$ on stress distribution for a bending is not so large compared with that of a

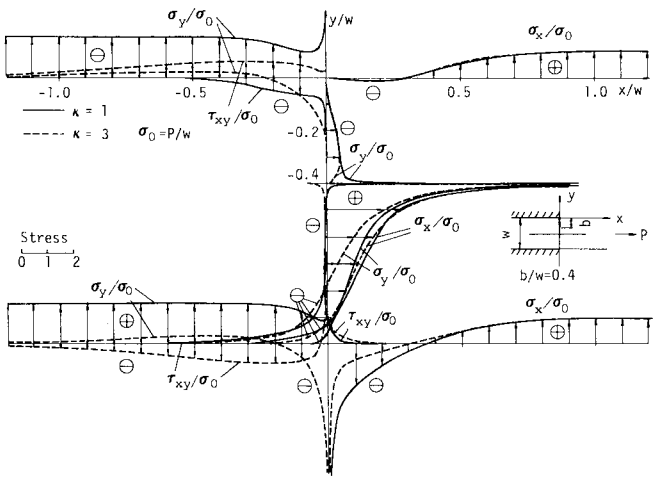

Fig. 6 Example of Stress Distribution under Tension (Crack Length $b/w=0.4$)

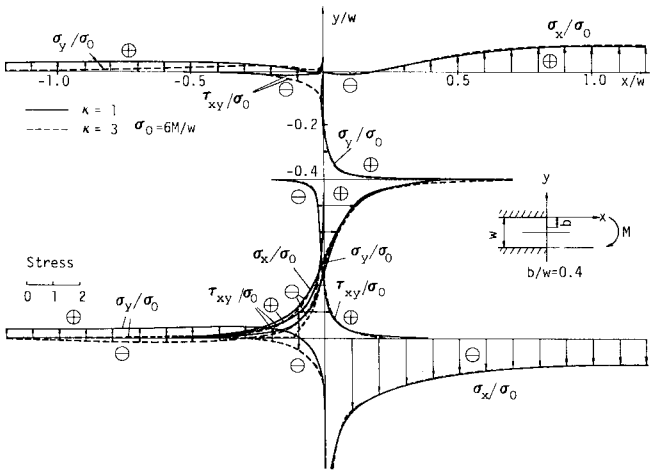

Fig. 7 Example of Stress Distribution under Bending (Crack Length $b/w=0.4$).

uniaxial tension. This is because the stress condition becomes antisymmetric with respect to $x/y=-0.5$ in the embedded part and the deformation in the direction of the width w is small.

5. STRESS INTENSITY FACTOR

Stress intensity factors are obtained for a uniaxial tension and a bending in the plane. Once the complex stress function $\phi(\zeta)$ is obtained, stress intensity factors K_{I} and K_{II} for mode I and mode II respectively are calculated from the following equation,

$$K_{\mathrm{I}}-iK_{\mathrm{II}}=2\sqrt{\pi}\, e^{-0.5i\delta}\phi'(\zeta_1)/\sqrt{\omega''(\zeta_1)}$$

where ζ_1 is a coordinate on the unit circle corresponding to the tip of the crack and δ is an angle between the x axis and the crack. In this paper $\zeta_1=1$ and $\delta=3\pi/2$.

a) Uniaxial tension

The following nondimensional stress intensity factor is used,

$$F_{\mathrm{I}}+iF_{\mathrm{II}}=\frac{(W-b)^{1.5}(K_{\mathrm{I}}+iK_{\mathrm{II}})}{(W+2b)P\sqrt{\pi}}$$

Stress intensity factors are calculated for the unembedded strip in order to investigate the precision of the rational mapping function. The values are shown in Table 1 and by a dash-dot line in Fig. 8. Table 1 also shows values obtained by Benthem et al.[9] and Gross et al.[9]. It is found that our values agree well with their approximate values. Fig. 8 and Table 2 show values F_{I} and F_{II} for the embedded strip. The difference of values F_{I} and F_{II} between the embedded and unembedded strip can be found. Values F_{I} and F_{II} depend on a value κ and the dependence is larger for a short crack. The behaviour of F_{I} and F_{II} of $\kappa=1$ is different from that of $\kappa\neq1$. When b/w approaches 1.0 and $\kappa\neq1$, values of F_{I} and F_{II} approach 0.313 and -0.049 respectively. On the other hand, values of F_{I} and F_{II} for $\kappa=1$ approach 0.309 and -0.050 respectively. Values of F_{I} for a short crack are larger than those of F_{I} for the unembedded strip, but for a long crack values of F_{I} are smaller than those for the unembedded strip. This seems as the following fact : stress concentration of the stiffened end between L and M influences more on F_{I} of the embedded strip for a short crack. On the other hand, for a long crack the influence of the flexibility of the unembedded strip is larger than that of the embedded strip.

b) Bending in the plane

The following nondimensional stress intensity factor is used,

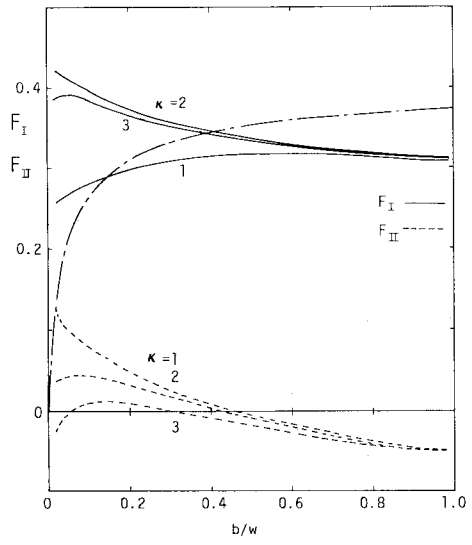

Fig. 8 Nondimensional Stress Intensity Factor under Tension.

Table 1 Nondimensional Stress Intensity Factor of an Unembedded Strip under Tension.

b/w	this paper (1)	Benthem et al. (2)	Gross, B. et al. (3)	Errors (2)-(1)/(1)	Errors (3)-(1)/(1)
0.02	0.149				
0.03	0.176				
0.04	0.197				
0.05	0.215	0.215	0.214	0.0 %	-0.47 %
0.10	0.268	0.268	0.267	0.0	-0.37
0.20	0.313	0.314	0.314	0.32	0.32
0.30	0.333	0.335	0.334	0.60	0.30
0.40	0.345	0.347	0.344	0.58	-0.29
0.50	0.353	0.354	0.354	0.28	0.28
0.60	0.359	0.359	0.359	0.0	0.0
0.70	0.364	0.364		0.0	
0.80	0.368	0.368		0.0	
0.90	0.371	0.371		0.0	
0.95	0.373	0.372		-0.27	
0.96	0.373	0.373		0.0	
0.97	0.374	0.373		-0.27	
1.00		0.374			

Table 2 Nondimensional Stress Intensity Factor under Tension.

	F_I					F_{II}				
b/w	κ=1.0	κ=5/3	κ=2.0	κ=2.5	κ=3.0	κ=1.0	κ=5/3	κ=2.0	κ=2.5	κ=3.0
0.02	0.256	0.424	0.421	0.405	0.386	0.127	0.064	0.037	0.002	-0.026
0.03	0.260	0.418	0.416	0.404	0.389	0.107	0.061	0.039	0.011	-0.011
0.04	0.263	0.413	0.413	0.403	0.391	0.102	0.061	0.041	0.016	-0.055
0.05	0.267	0.409	0.410	0.402	0.391	0.099	0.062	0.043	0.019	-0.001
0.10	0.280	0.393	0.395	0.391	0.385	0.080	0.058	0.044	0.025	0.010
0.20	0.298	0.371	0.372	0.370	0.367	0.049	0.042	0.032	0.020	0.010
0.30	0.308	0.356	0.357	0.356	0.354	0.025	0.024	0.017	0.009	0.002
0.40	0.314	0.345	0.345	0.345	0.343	0.007	0.008	0.003	-0.003	-0.008
0.50	0.317	0.336	0.337	0.336	0.335	-0.007	-0.007	-0.010	-0.014	-0.018
0.60	0.318	0.329	0.330	0.329	0.328	-0.019	-0.019	-0.021	-0.024	-0.026
0.70	0.317	0.323	0.324	0.323	0.323	-0.028	-0.030	-0.031	-0.033	-0.034
0.80	0.314	0.318	0.319	0.319	0.318	-0.038	-0.039	-0.039	-0.040	-0.041
0.90	0.311	0.314	0.315	0.315	0.314	-0.046	-0.046	-0.046	-0.047	-0.047
0.95	0.310	0.313	0.313	0.313	0.313	-0.050	-0.049	-0.049	-0.049	-0.049
0.96	0.309	0.312	0.313	0.313	0.313	-0.050	-0.049	-0.049	-0.049	-0.049
0.97	0.309	0.312	0.313	0.313	0.313	-0.050	-0.049	-0.049	-0.049	-0.049

$$F_I + iF_{II} = (W-b)^{1.5}(K_I + iK_{II})/(6M\sqrt{\pi})$$

Values F_I and F_{II} for the unembedded strip are shown in Table 3 and by a dash-dot line in Fig. 9. In Table 3, approximate values of Benthem et al.[9] and Gross et al.[9] are also shown. Our values agree well with those of Gross et al. Fig. 9 and Table 4 show values F_I and F_{II} for the embedded strip. When b/w approaches to 1.0 and $\varkappa \neq 1$, values of F_I and F_{II} approach to values of 0.312 and -0.050 respectively. On the other hand, values of F_I and F_{II} for $\varkappa=1$ approach to 0.308 and -0.052 respectively. The influence of $\varkappa$ on F_I and F_{II} is different between $\varkappa=1$ and $\varkappa \neq 1$, but it is not so large compared with that of a uniaxial tension. This is because the external force is antisymmetric with respect to $x/w=-0.5$ and the deformation in the direction of the width w is small compared with a uniaxial tension. When a crack length is less than about $b/w=0.1$, values of F_I are larger than those of the unembedded strip. However it is the reverse when b/w is larger than about $b/w=0.1$. This is because the unembedded strip is more flexible than that of the embedded strip for a long crack. However for a short crack, the influence of stress concentration at the stiffened end is larger.

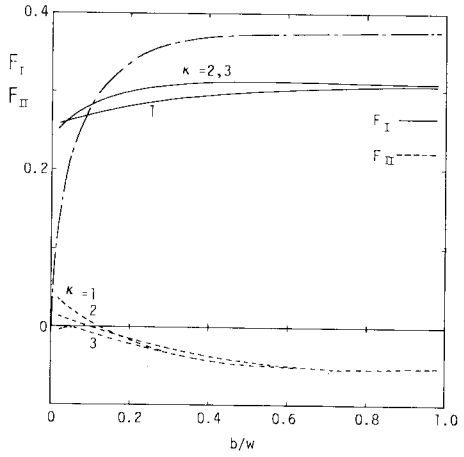

Fig. 9 Nondimensional Stress Intensity Factor under Bending.

Table 3 Nondimensional Stress Intensity Factor of an Unembedded Strip under Bending.

b/w	this paper (1)	Benthem et al. (2)	Gross,B. et al. (3)	Errors (2)-(1)/(1)	Errors (3)-(1)/(1)
0.02	0.151				
0.03	0.180				
0.04	0.203				
0.05	0.222	0.221	0.222	-0.45%	0.0%
0.10	0.283	0.281	0.282	-0.71	-0.35
0.20	0.338	0.334	0.338	-1.18	0.0
0.30	0.361	0.355	0.360	-1.66	-0.27
0.40	0.371	0.360	0.370	-2.96	-0.27
0.50	0.374	0.370	0.374	-1.07	0.0
0.60	0.375	0.373	0.374	-0.53	-0.27
0.70	0.375	0.373		-0.35	
0.80	0.374	0.374		0.0	
0.90	0.374	0.374		0.0	
0.95	0.374	0.374		0.0	
0.96	0.374				
0.97	0.375				
0.98	0.376				

Table 4 Nondimensional Stress Intensity Factor under Bending.

	F_I					F_{II}				
b/w	κ=1.0	κ=5/3	κ=2.0	κ=2.5	κ=3.0	κ=1.0	κ=5/3	κ=2.0	κ=2.5	κ=3.0
0.02	0.260	0.260	0.258	0.255	0.252	0.034	0.019	0.012	0.003	-0.005
0.03	0.260	0.263	0.262	0.260	0.258	0.028	0.016	0.011	0.004	-0.002
0.04	0.262	0.267	0.266	0.265	0.263	0.024	0.014	0.010	0.004	-0.001
0.05	0.263	0.271	0.270	0.269	0.268	0.021	0.012	0.008	0.003	-0.002
0.10	0.270	0.284	0.284	0.284	0.283	0.006	0.002	-0.001	-0.004	-0.008
0.20	0.281	0.300	0.301	0.301	0.300	-0.017	-0.016	-0.018	-0.020	-0.022
0.30	0.289	0.307	0.308	0.309	0.308	-0.034	-0.029	-0.030	-0.032	-0.034
0.40	0.295	0.311	0.312	0.312	0.312	-0.044	-0.039	-0.039	-0.041	-0.042
0.50	0.299	0.312	0.313	0.313	0.313	-0.049	-0.045	-0.045	-0.046	-0.047
0.60	0.303	0.312	0.312	0.313	0.312	-0.051	-0.048	-0.049	-0.049	-0.050
0.70	0.305	0.311	0.312	0.312	0.312	-0.052	-0.050	-0.051	-0.051	-0.052
0.80	0.306	0.311	0.311	0.311	0.311	-0.052	-0.051	-0.051	-0.052	-0.052
0.90	0.307	0.311	0.311	0.311	0.311	-0.053	-0.052	-0.052	-0.052	-0.052
0.95	0.308	0.311	0.311	0.311	0.311	-0.053	-0.052	-0.051	-0.051	-0.052
0.96	0.308	0.311	0.311	0.312	0.311	-0.053	-0.051	-0.051	-0.051	-0.051
0.97	0.308	0.311	0.312	0.312	0.312	-0.052	-0.050	-0.050	-0.050	-0.050

6. CONCLUSION

A rational mapping function of fractional expressions is represented by Eq. (5) for a finite and a simple connected region. The general solution of a mixed boundary value problem is given by Eqs. (6) and (10). Stress intensity factors for the unembedded strip agree well with those of Benthem et al. and Gross et al. The influence of κ is larger for a short crack than for a long crack. It is larger for a uniaxial tension than for a bending in the plane. Stress distribution and stress intensity factor for $\kappa=1$ are different from those of $\kappa=1$. Stress distribution of the embedded part is different before and after the occurrence of a crack. When $\kappa=1$, stress in the embedded part after the occurrence of a crack is larger than that before the occurrence of a crack and larger than the nominal stress σ_0. The influence of stress concentration on stress intensity factor is larger for a short crack. For a long crack the influence of flexibitity of strip is larger.

REFERENCES

1) Hasebe, N. and Miura, M. : Stress Analysis of Cracks Emanating from Both Stiffened ends of an Embedded Strip, Transactions of the Japan Society of Mechanical Engineers (Series A), Vol. 47, No. 423, pp. 1129~1136, 1981.
2) Hasebe, N. : Uniform Tension of a Semi-Infinite Plate with a Crack at an End of a stiffened Edge, Ingenieur Archiv, Vol. 48, pp. 129~141, 1979.
3) Hasebe, N. : An Edge Crack in a Semi-Infinite Plate Welded to a Rigid Stiffener, Proceedings of the Japan Society of Civil Engineers, No. 314, pp. 149~157, 1981.
4) Delale, F. and Erdogan, F. : The Crack Problem for a Half Plane Stiffened by Elastic Cover Plates, International Journal Solids Structures, Vol. 18, No. 5, pp. 381~395, 1982.
5) Hasebe, N. : Bending of Strip with Semielliptic Notches or Cracks, Journal of the Engineering Mechanics Division, Proceedings of the American Society of Civil Engineers, Vol. 104, No. EM 6, pp. 1433~1450, 1977.
6) Hasebe, N. and Inohara, S. : Stress Analysis of a Semi-Infinite Plate with an oblique Edge Crack, Ingenieur Archiv, Vol. 49, pp. 51~62, 1980.
7) Hasebe, N., and Takemura, M. : Crack at Joint of Strip and Semi-Infinite Plate, Engineering Fracture Mechanics, Vol. 15, No. 1-2, pp. 45~53, 1981.
8) Muskhelishvili, N. I. : Some Basic Problems of Mathematical Theory of Elasticity, 2nd ed., Noordhoff, Netherlands, 1963.
9) Benthem, J. P. and Koiter, W. T. : Methods of Analysis and Solutions of Crack Problems, Mechanics of Fracture, Vol. 1, G. C., Sih ed., Leyden, Netherlands, 1973.

(Received March 8 1985)